Parity and Time Reversal Studies at STAR

A. Chikanian and J. Sandweiss

July 7, 1999

Contents

List of Figures

1. Introduction

A recent publication [1] raises the interesting hypothesis that in high energy heavy ion collisions, such as at RHIC there can be violations of parity (P) and time reversal (T) at the level of the strong interaction. Since that publication there have been additional discussions at the RIKEN BNL theory center and further work by Kharzeev [2] and Gyulassy [3].

Stimulated by these ideas, we have begun to explore the possible ways in which such effects could be studied using the STAR detector at RHIC. The present note is a progress report on these studies. We find that, at least as far as statistics is concerned, the STAR program can find the P, T violating effects predicted by the above considerations. The all important questions of experimental systematic errors remain to be analyzed although we believe, based on past related experience, that they will not turn out to be a "show stopper". The present report deals only with these statistical aspects, although future work will soon be done to address these experimental systematic errors. A number of Star collaborators have also expressed interest in these studies and one of these, Jim Thomas, has established a STAR Parity mailing list [4] and a WEB page for a STAR Parity discussion group [5].

An important aspect of the effects hypothesized is that they originate through a spontaneous symmetry breaking mechanism. This can result in the effects randomly varying from event to event resulting in an apparent lack of violation when the "results" are summed over a large number of events. This aspect will be explained in some detail in the succeeding sections. This feature has the consequence that the usual methods for detecting such a violation would fail to show an effect. For example a parity odd operator would still have a zero expectation value when evaluated for a large sample of events.

Not surprisingly, the parameters which do add, with the same sign, from event to event are second order in the violation. In the past, to our knowledge, such parameters have never been experimentally studied. This raises the interesting possibility that such P,T violating effects may have already occured in high energy collisions e.g. at CDF, LEP or SLD. One purpose of the present note is to encourage the

experimenters at these facilities to examine their existing data for such phenomena.

We have examined three different variables as signatures of the effects. In the sections below we present our studies of these three variables. Of these, only one, the Gyulassy "twist tensor", appears to be useful, at least for the initial studies. In the later sections of this report we focus mainly on the twist tensor but also add our analyses of the other parameters for completeness.

In evaluating the size of the effects and the necessary sample size, we have utilized a model of the effect which attempts to make realistic estimates of the combinatoric dilution and the "observability" of the violation. This model is described in the next section.

2. The Simulation Model

The theory [1] predicts that a domain is formed in the collision volume which has a finite value of $< \vec{E} \cdot \vec{B} >$, where the fields are chromodynamic fields. Such an expectation value manifestly violates P and T. In an event, the violation shows up via the effects these fields have on the trajectories of (colored) quarks passing through the domain. Effects can also occur if pions pass through the domain walls [2]. Kharzeev [2] has estimated these effects by estimating the impulse the fields would impart to a quark traversing the domain. He finds the chromo $\vec{E}$ field would yield an impulse of 30 MeV/c for a quark crossing the diameter of the domain. The chromo $\vec{B}$ field would give a transverse impulse of the same value to a (relativistic) quark traversing the diameter of the domain perpendicularly to the chromomagnetic field.

These impulse values are minimum estimates and Kharzeev estimates that the actual effects will lie between these and values with four times greater impulse.

The finite chromo $\vec{E} \cdot \vec{B}$ arises in the theory when the collision volume undergoes the phase transition to the hadronic from the partonic state. In each event, the domain may be formed differently so that, for example, the chromo $\vec{E}$ points in a different random direction. However, a key point is that whatever the direction of the chromo $\vec{E}$, the direction of the chromo $\vec{B}$ is in the same direction.

In our simulation model, we place a spherical domain containing an electromagnetic $\vec{E}$ and electromagnetic $\vec{B}$, parallel to one another but otherwise randomly oriented in each event. We locate the domain with its center randomly chosen inside the interaction volume but constrained so that the domain lies completely within the interaction volume.

We choose the interaction volume to be spherical with a radius of 5 Fermi and we choose the domain to have a radius of 2 Fermi. Particles are then generated with a uniform distribution throughout the interaction volume. The particles are generated either exactly as HIJING predicts or in a similar but simpler fashion which will be detailed below. The particles are tracked through the interaction volume.

If they traverse the domain, the impulses they receive from the $\vec{E}$ and $\vec{B}$ fields are calculated from the Lorentz force they experience taking the geometric effects into account (track length in the domain, orientation with respect to the fields). The magnitudes of the electromagnetic $\vec{E}$ and $\vec{B}$ are chosen to give the same impulse to a charge 1 particle as the chromo fields would have given to a quark.

The choice of a 5 Fermi radius is meant to be a "typical" value for central RHIC collisions. The choice of 2 Fermi for the domain radius comes from discussions with theoretical colleagues who felt that if the domains are formed at all they will at least have this size.

As noted above, the kinematic parameters of the generated particles are chosen according to two different schemes which are enumerated below. For both schemes, the particle kinematic parameters after the initial choice are "smeared" to represent experimental resolution. We smear the x, y, and z momentum components (without correlation) in a Gaussian fashion with standard deviations $\Delta p_x/p = \Delta p_y/p = \Delta p_z/p = .02$. In addition, because of the acceptance limitations of the STAR detector we generate particles inside a limited range of y and p_t. These are slightly different for the two types and are listed below.

For both schemes, after the tracks are generated and smeared the final accepted transverse momentum must be greater than 250 MeV and the space angle must be greater than 22°.

1. In the first scheme we just take the HIJING generated particles for zero impact parameter. Because of technical considerations (mostly disk space), this approach is limited (for the present time) to a sample size of 40,000 events. For the particles saved, before smearing, we limit the sample to $p_t > 150 MeV$ and space angle $\theta > 15°$. To "simulate" the loss of efficiency for identifying tracks which are nearly parallel, we also require a minimum opening angle (space) of greater than 10 mr, $\theta_{open} > 10$ mr.

   For reference, some of the characteristics of the HIJING events are shown in figure 2.1. For simplicity, just the deflections due to the imbedded magnetic field are shown. The histogram describes the deflections in the P,T violating domain for those particles that cross the domain. All particles which do not cross the domain have zero deflection and are not plotted. In the full simulations, of course, the vector sum of the magnetic and electric impulses is properly calculated and the deflections calculated accordingly.

2. In the "fast" simulation studies we generate$\sim$ 1000 positive pions and $\sim$ 1000 negative pions, each chosen independently with rapidity and transverse momentum values selected so as to reproduce the rapidity and transverse momen-

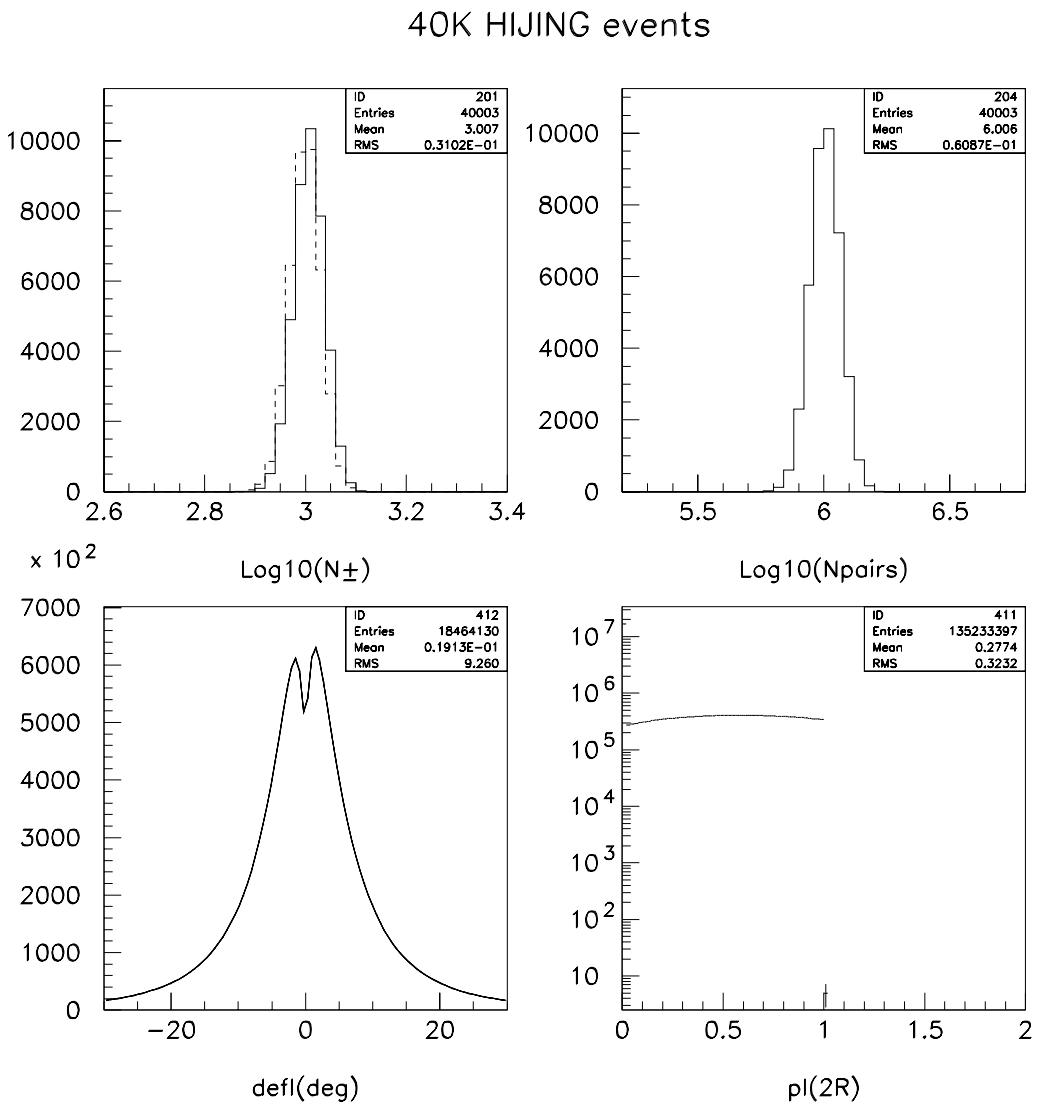

Figure 2.1: The four panels show for the HIJING events: the number of positive and negative tracks per event (dashed line for negative), the number of pairs per event, the deflection for particles passing through the P,T violating domain due to the "imbedded" magnetic field for a domain with $3\times$ the minimum deflection [2], and the distribution of path lengths through the P,T violating domain (in units of the maximum path length $2R$).

tum spectrum predicted by HIJING for all pions. We assume that the rapidity and transverse momentum are uncorrelated here so y and p_t are chosen independently. Here the saved particles before smearing must have $p_t > 250 MeV$ and y between ± 1.6. This makes a small error in that it neglects particles with p_t below 250 MeV which after smearing would have $p_t > 250 MeV$. The effect is, however, negligible and this procedure is convenient. Here also we require a minimum opening angle of 10 mr, $\theta_{open} > 10$ mr.

We show some characteristics of the events generated with this approach, figure 2.2.

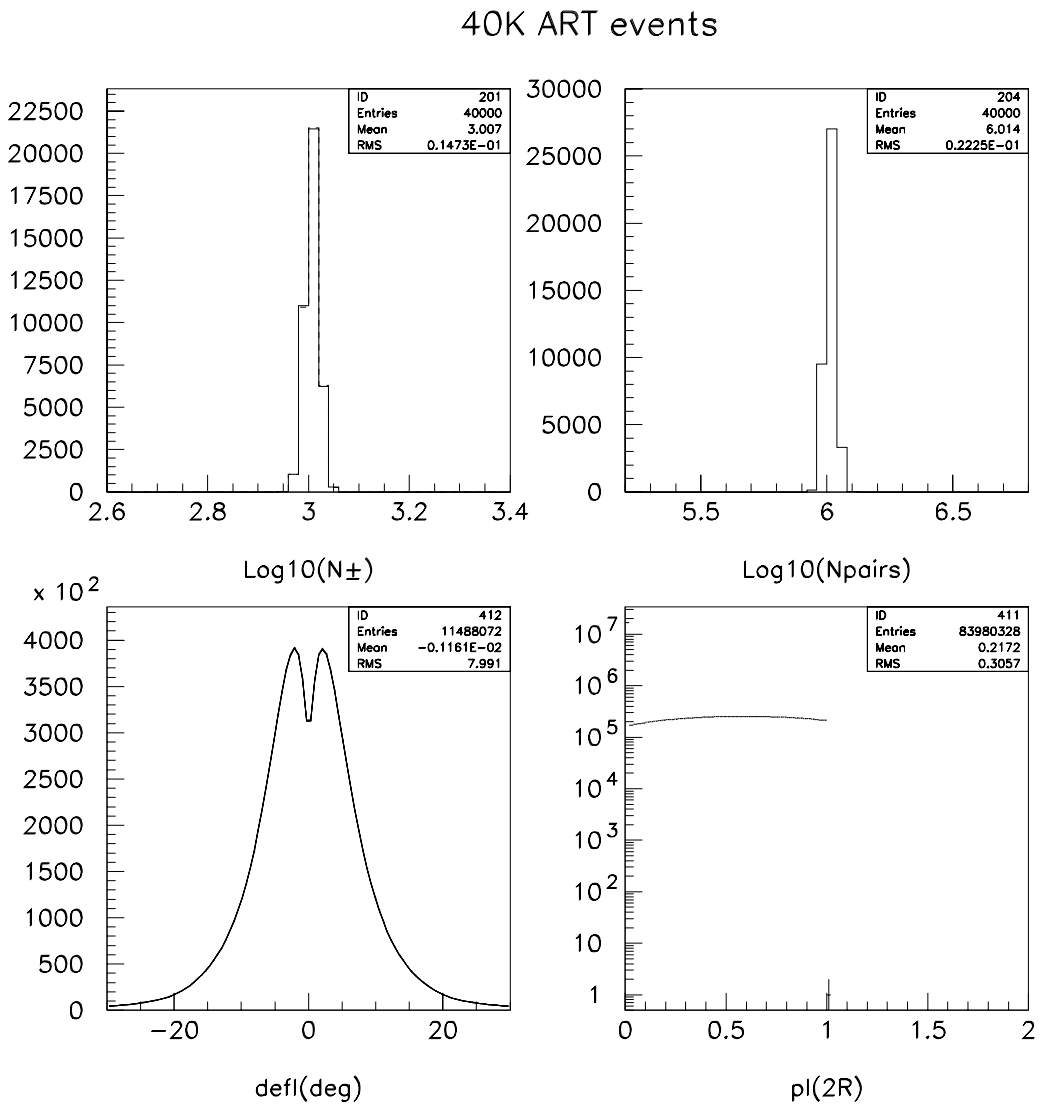

Figure 2.2: The four panels show for the fast simulation events ("artificial" events): the number of positive and negative tracks per event, the number of pairs per event, the deflection due the the "imbedded" magnetic field for a domain with $3\times$ the minimum deflection [2], and the distribution of path lengths through the CP violating domain (in units of the maximum path length, $2R$).

3. The Twist Tensor

Gyulassy [3] has proposed a variable, the twist tensor. We use a somewhat different normalization of the tensor (which does not change its transformation properties) and has the advantage of limiting the maximum magnitude to unity. Specifically, we define T_{ij} via:

$$T_{i,j} = (\frac{1}{N_{pairs}}) \sum_{pairs} \frac{\vec{P_+} \times \vec{P_-} \cdot \hat{n_i}}{\mid \vec{P_+} \mid\mid \vec{P_-} \mid} \frac{(\vec{P_+} - \vec{P_-}) \cdot \hat{n_j}}{\mid \vec{P_+} - \vec{P_-} \mid} \tag{3.1}$$

In (3.1) $\vec{P_+}$ and $\vec{P_-}$ refer to the momenta of the positively and negatively charged particles and $\hat{n_i}$ refers to the unit vector along the x, y, or z axis (axes labeled by i, j). In all of the following we use the convention that the z axis is along the beam direction.

Gyulassy [3] points out that

$$TR(T_{i,j}) = T_{xx} + T_{yy} + T_{zz} = 0 \tag{3.2}$$

From which

$$T_{zz} = -(T_{xx} + T_{yy}) \tag{3.3}$$

The components of $T_{i,j}$ are odd under the parity transformation (P) and even under charge conjugation (C) and thus are odd under T (given the TCP theorem). Their average values can be thought of as measures of the correlation between the handedness bias induced by the magnetic field and the charge-momentum bias induced by the electric field. Thus the effect of the P,T violation should have the same sign on a given component of $T_{i,j}$ in each event since the sign of the effect depends on the relative orientation of $\vec{E}$ and $\vec{B}$, which is always the same.

Furthermore, if P and T are conserved in the interaction, we would expect the average value of any component of $T_{i,j}$ to be zero when averaged over a large number of events.

In addition, if there is azimuthal symmetry around the beam direction, T_{xy} and T_{yx} must have the same average value.

This is verified for our simulation in the case of the fast simulation but for an unkown reason (at present) it is not quite true for the HIJING generated events.

3.1 HIJING Results

The next series of figures show the results for the HIJING events. Figure 3.1 shows the distrubutions for the 9 elements of $T_{i,j}$ for 1000 HIJING events.

Figure 3.2 shows the distributions in the average values of the elements of $T_{i,j}$ for an ensemble of 400 subsamples, each of 100 events. In other words, $T_{i,j}$ is averaged over all the pairs in a subsample of 100 events, and these subsample averages are histogrammed. In this figure, the value of the parity violating fields are chosen to give a deflection of $3\times$ the minimum deflection [2].

From figure 3.2 we see that the relation 3.3 is satisfied. We also see statistically significant P,T violation in the mean value of the T_{zz} distribution (and of course in the T_{xx} and T_{yy} distributions, given 3.3.

To see how the effects depend on the values of the P, T violating $\vec{E}$ and $\vec{B}$ fields we show figure 3.3 which is the same as figure 3.2 except that the P,T violating fields are set to zero.

Here we see that all elements of $T_{i,j}$ except $T_{x,y}$ and $T_{y,x}$ suitably average to zero, as they should. Furthermore, for azimuthal symmetry around the beam axis (which is assumed in HIJING) the x and y directions are equivalent so $T_{x,y}$ should equal $T_{y,x}$. The fact that a nonzero mean for $T_{x,y}$ obtains and that the distributions of $T_{x,y}$ and $T_{y,x}$ are not the same is not understood at this time. It would seem to be a bug in HIJING (or in the way we are using it!).

In any case, the effect does properly vanish for the diagonal elements. As we shall see, in the fast simulation study this discrepancy does not occur and the P,T violating effects are similar for the diagonal elements.

For the present we assume that the $T_{x,y}$ and $T_{y,x}$ results are not correct with the HIJING events, but that the diagonal elements are good measures of the size of the effect we could expect.

Figure 3.4 shows a summary of the results for the diagonal elements.

From figure 3.4 we see that a statistically significant observation of the minimum effect could just about be made with 40,000 events (assuming HIJING). The minimum effect shifts the peak by about half its standard deviation. An additional test

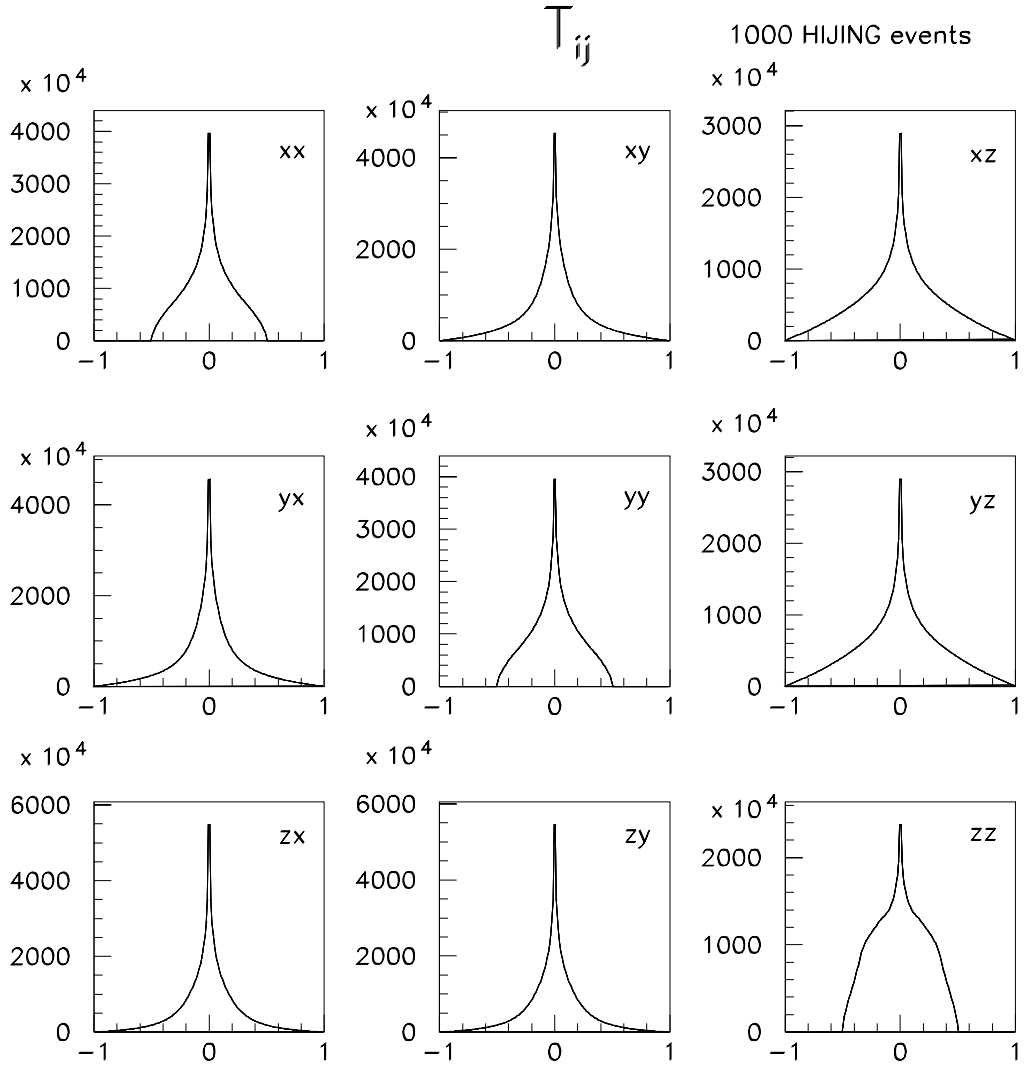

Figure 3.1: The distribution of the elements of $T_{i,j}$ for 1000 HIJING events.

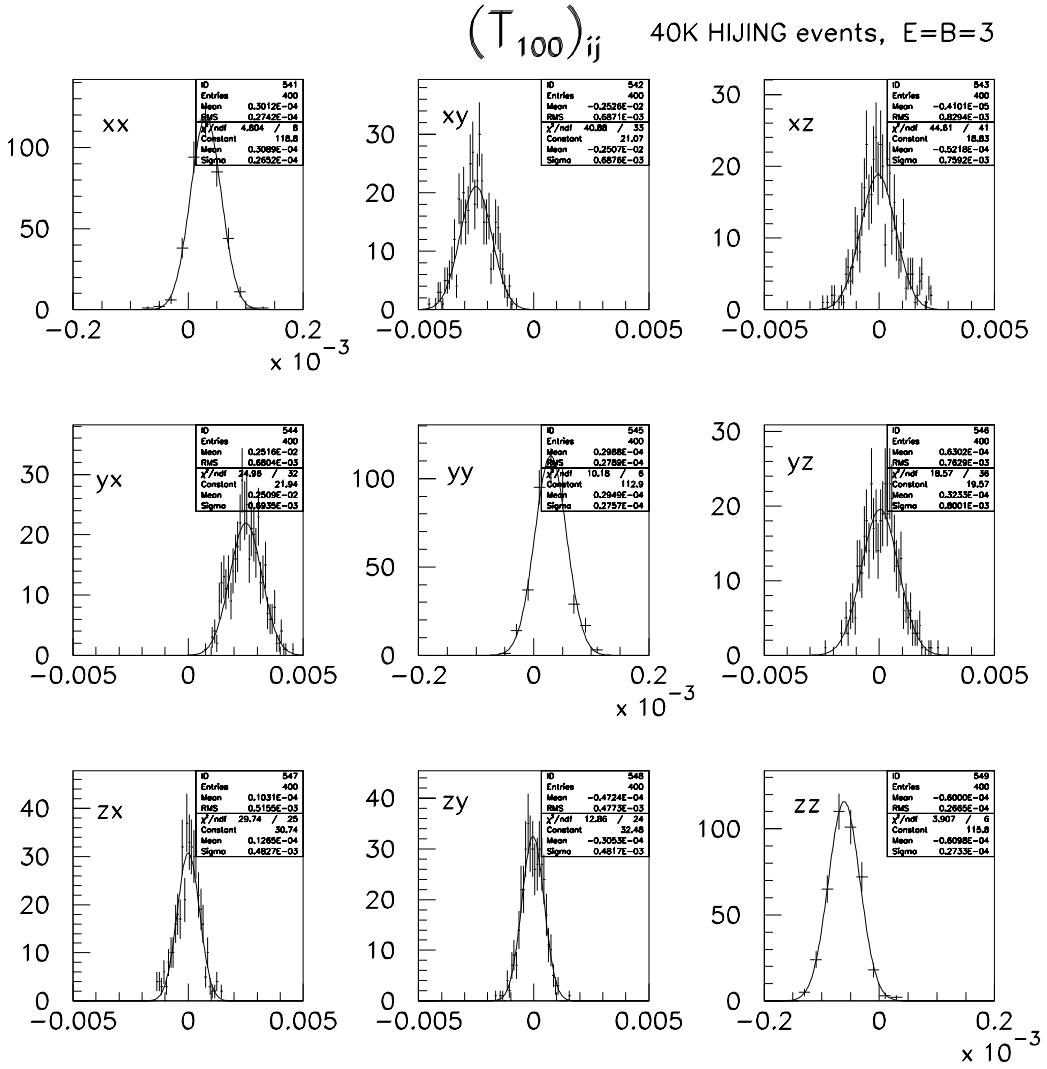

Figure 3.2: The distributions of the $T_{i,j}$ averaged over subsamples of 100 events. Here the P,T violating fields are chosen to give deflections of 3$\times$ the minimum expected deviation.

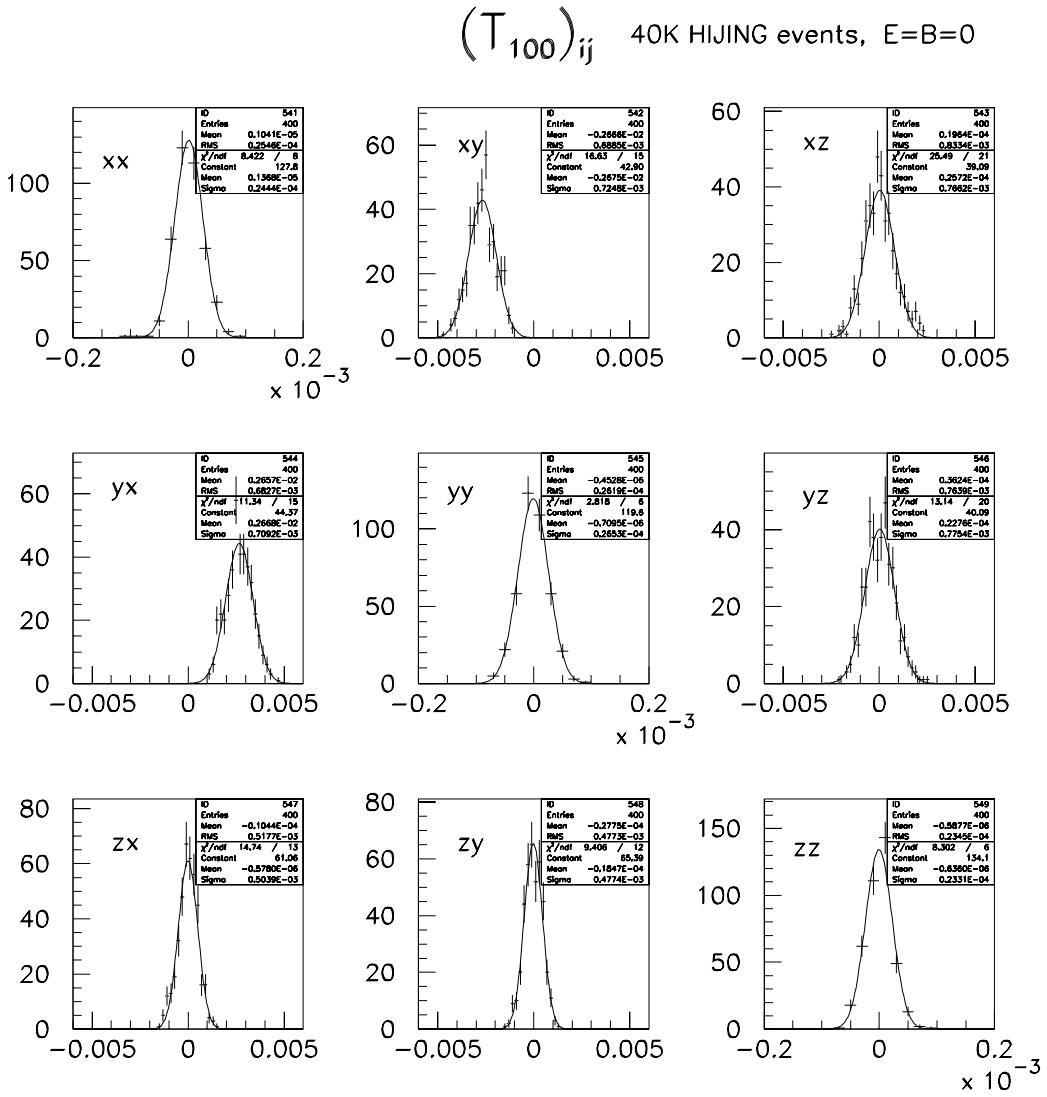

Figure 3.3: The distributions of the $T_{i,j}$ averaged over subsamples of 100 events. Here the P,T violating fields are chosen to be zero.

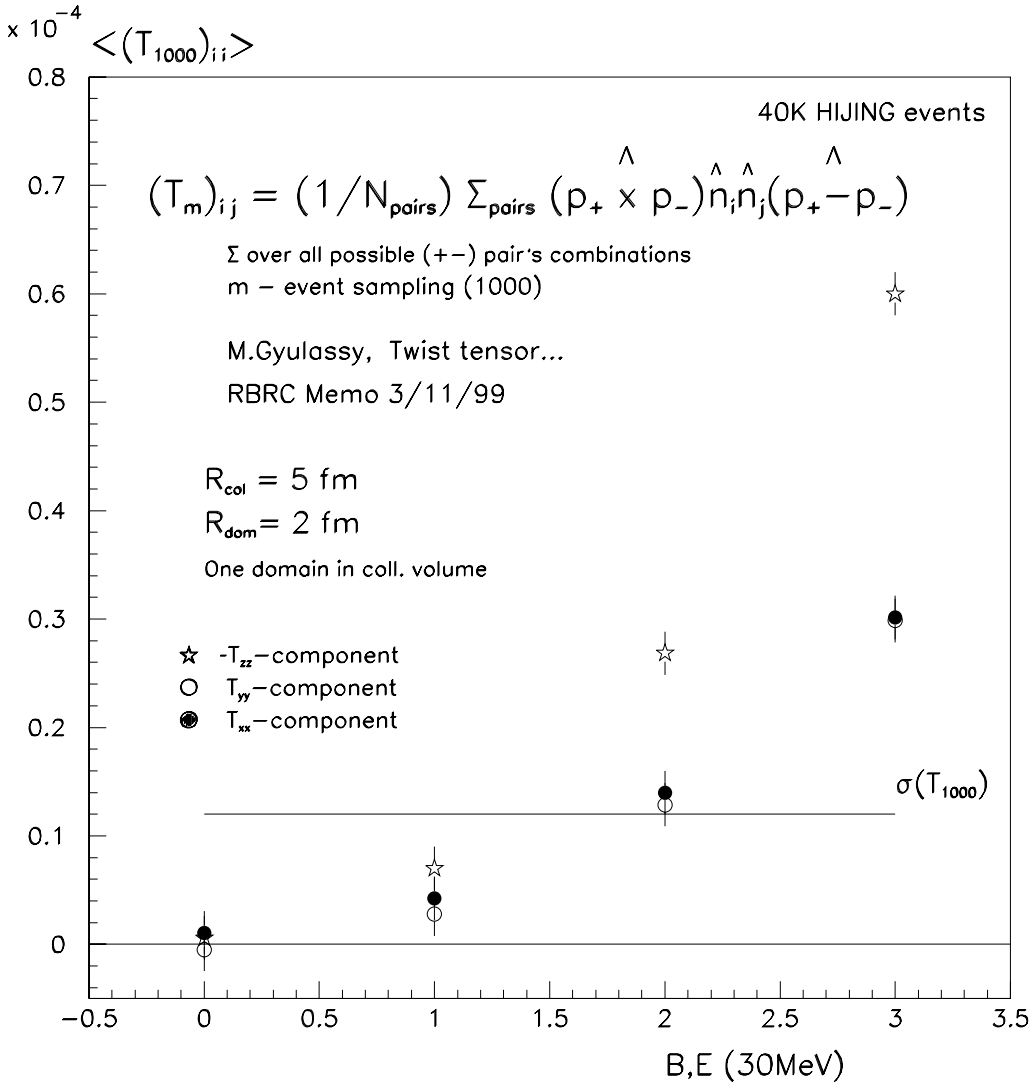

Figure 3.4: The average values of the diagonal elements of $T_{i,j}$ for various factors of the minimum P,T violating fields (in terms of the minimum value). The horizontal line shows the standard deviation of the width of the distribution of averages of 1000 event subsamples, calculated for a total sample of 40,000 events. The vertical lines on the points indicate the standard deviations of the averages.

for the correctness of the measurement will be the check of equation 3.3.

However, the T_{xx} and T_{yy} components also contain additional information on the P,T violation. The diagonal components of $T_{i,j}$ have some correlation so to study the statistical advantage of using all three, we have plotted the quantity $T_{xx}+T_{yy}-T_{zz}$. This is shown in figure 3.5.

From figure 3.5 we see that the effect is substantial. Statistically, the P,T violation shows up at more than 4 standard devistions from zero.

From figures 3.4 and 3.5 we conclude that statistically, an event sample of 40,000 central events has a significant ability to test the theory of reference [1]. The size of the effect would be around 10^{-5} in terms of the average values of relevant twist tensor components.

3.2 Fast Simulation Results

We have studied the twist tensor behavior for the events generated by our fast simulation (as described above in section 2). The next series of figures are the analogues of the ones shown in the previous section. With the fast simulation we can analyze much larger event samples. However, to compare with the HIJING results we show here results calculated with the same number of events (40,000) as we had for the HIJING studies. As can be seen from the plots, this number is actually sufficient to establish the statistical requirements of the measurement. The larger samples calculated agree with the conclusions drawn from the 40,000 event summaries.

Figure 3.6 shows the distribution of the nine components of $T_{i,j}$ for 1000 fast simulation events (so-called artificial events).

Figure 3.7 shows the distribution of the average values of the components of $T_{i,j}$ for subsamples of 100 events. The total number of events is 40,000. For this figure the magnitude of the P,T violating fields has been taken to be $3\times$ the minimum value.

As we did for the HIJING events, we test the simulation by calculating the average values of $T_{i,j}$ for the case with no P,T violating fields. These results are shown in figure 3.8.

We see that for these fast simulation events for zero P,T violating fields, each component of $T_{i,j}$ has a zero average value (within statistics for the calculation). This supports the hypothesis that there is some error in the HIJING simulation which shows nonzero $< T_{x,y} >$ and $< T_{y,x} >$.

The effect of the P,T violating fields is somewhat smaller for the fast simulation

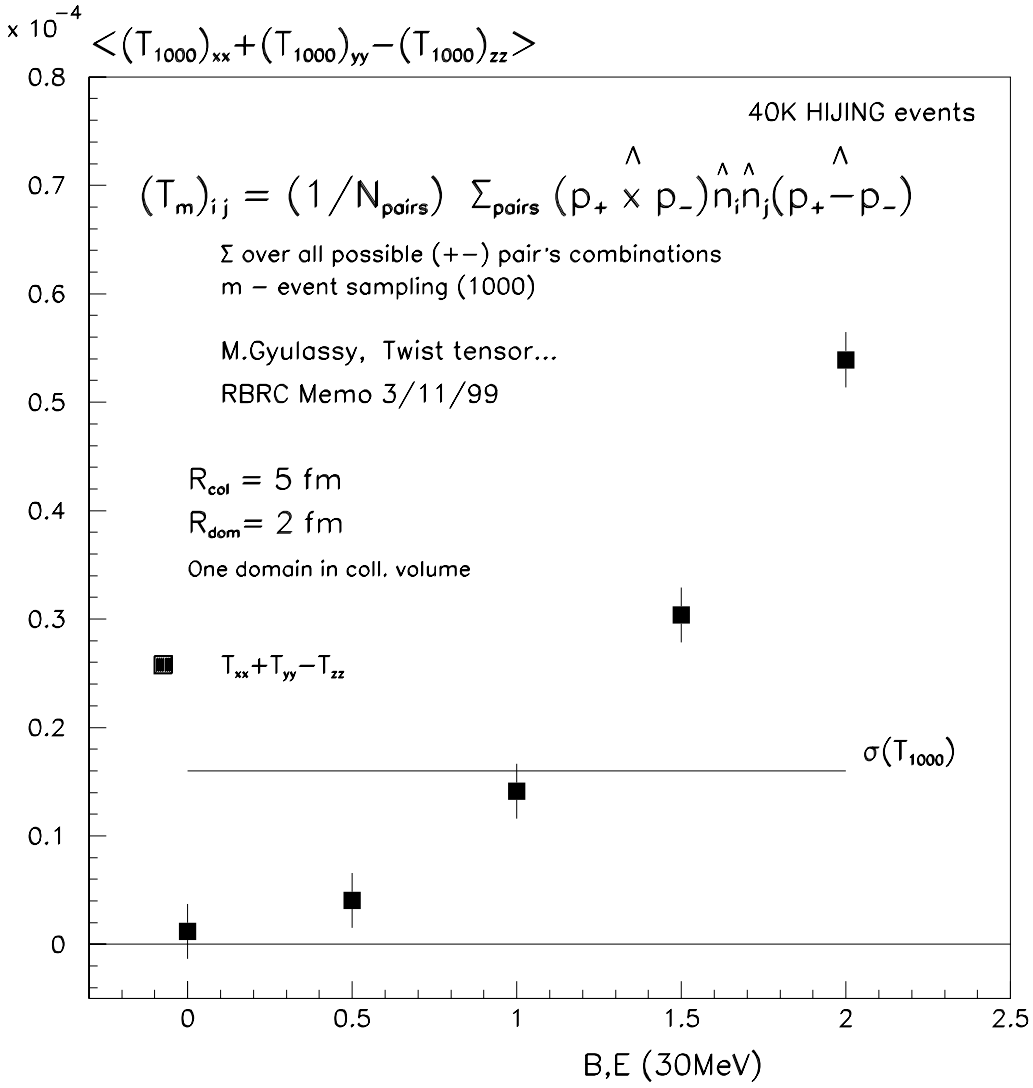

Figure 3.5: The average values of the sum $T_{xx} + T_{yy} - T_{zz}$ for various factors of the P,T violating fields (in terms of the minimum value). The horizontal line shows the width of the distribution of averages for 1000 event subsamples, calculated for a total sample of 40,000 events. The vertical lines indicate the standard deviations of the averages.

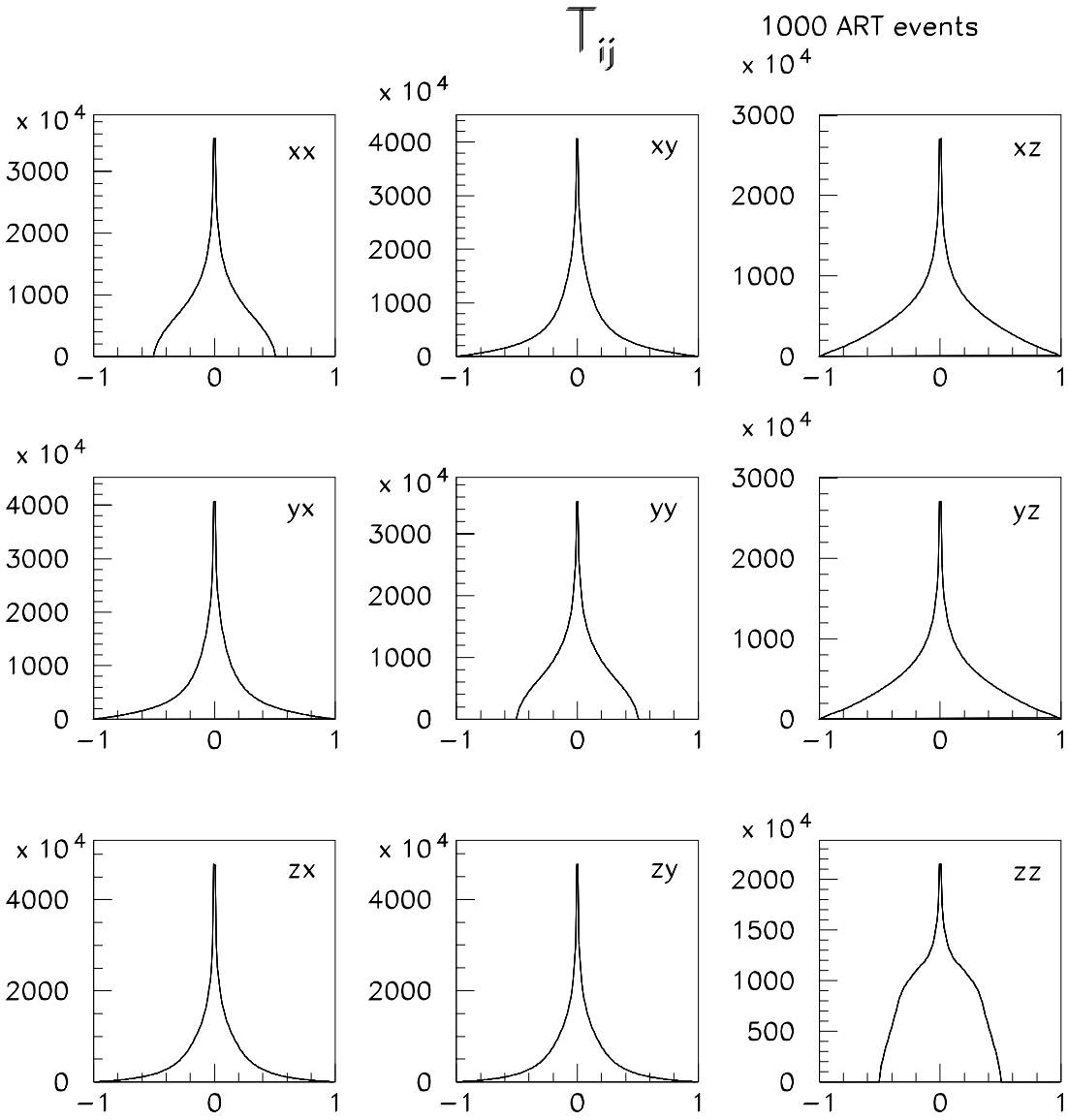

Figure 3.6: The distribution of the nine components of $T_{i,j}$ for 1000 fast simulation events.

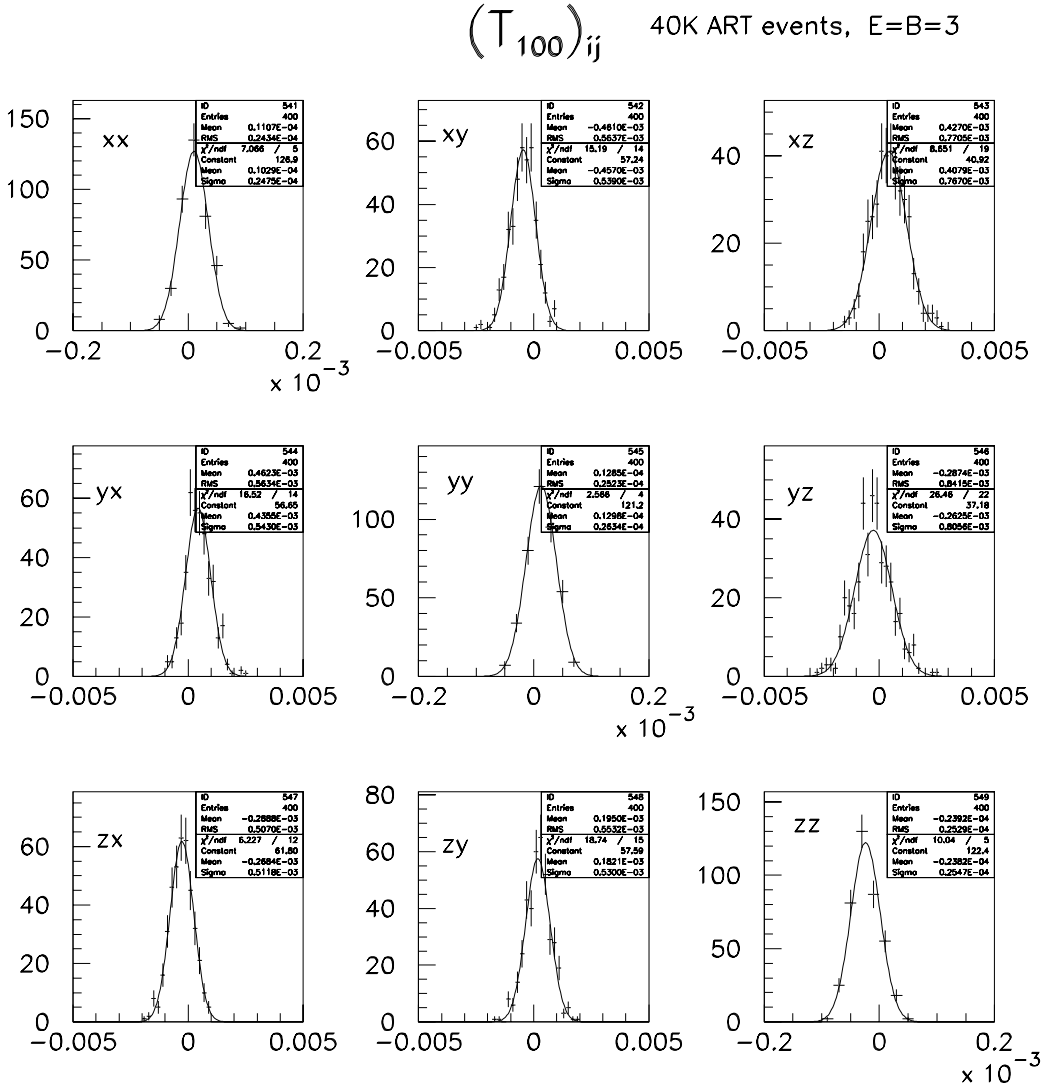

Figure 3.7: The distribution of the averages of the components of $T_{i,j}$ for 100 event subsamples of the fast simulation events. The total number of events is 40,000. The P,T violating fields are 3$\times$ the minimum value.

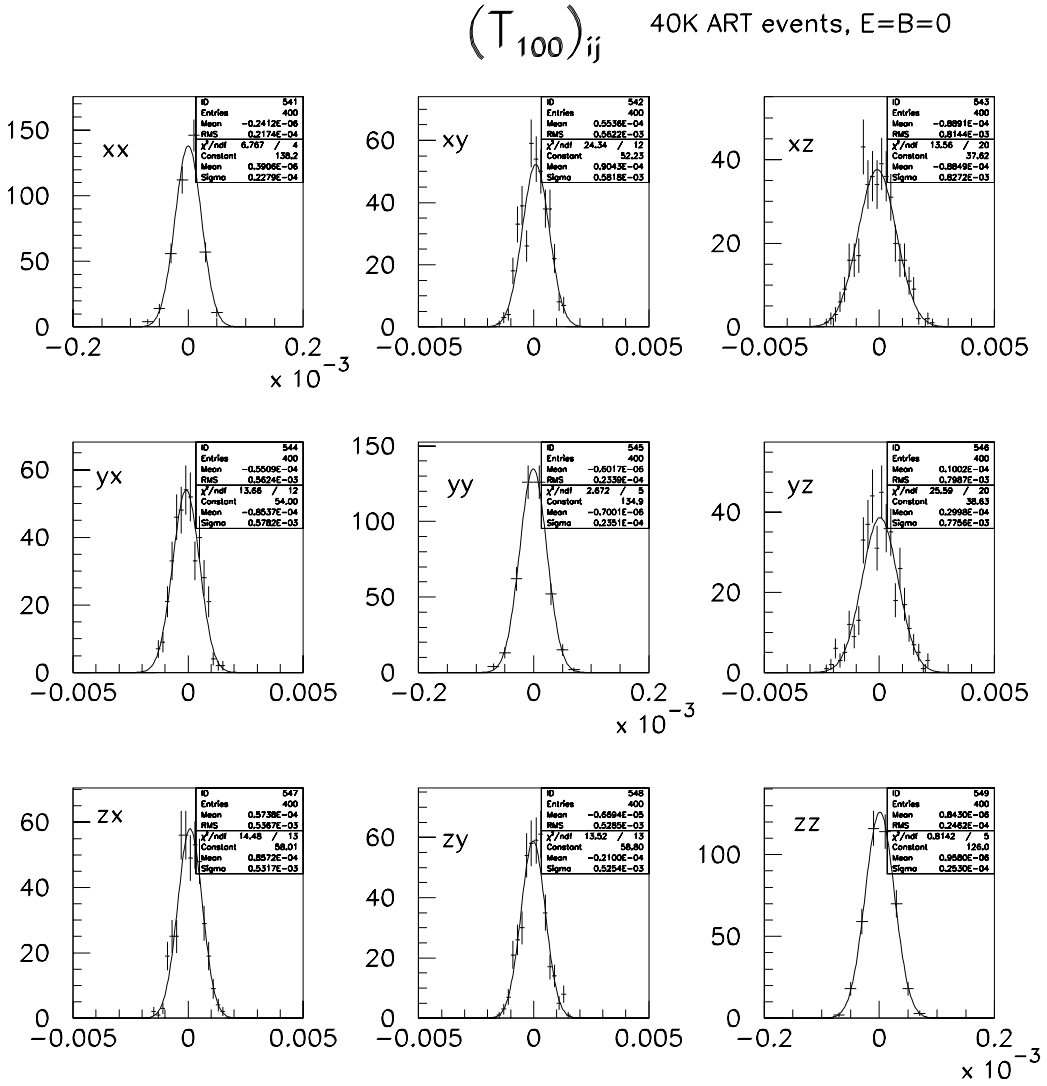

Figure 3.8: The distributions of the $T_{i,j}$ averaged over subsamples of 100 events, with the P,T violating fields set to zero. The total number of events is 40,000.

events as compared to the HIJING events (for the diagonal components). The effect is summarized in figure 3.9 which shows the average values of the diagonal components of $T_{i,j}$ for subsamples of 1000 events, for a total number of 40,000 events, for different magnitudes of the P,T violating fields.

Comparing figure 3.9 with figure 3.4 we see that the effect of the P,T violating fields are somewhat less in the case of the fast simulation events. The minimum value of the fields produces effects in T_{zz} which are about half of the width and about 2.5 standard deviations from zero. The combination of components $T_{xx} + T_{yy} - T_{zz}$ can be expected to show a larger effect, as was the case for the HIJING events. Figure 3.10 shows the result for this variable for the fast simulation events.

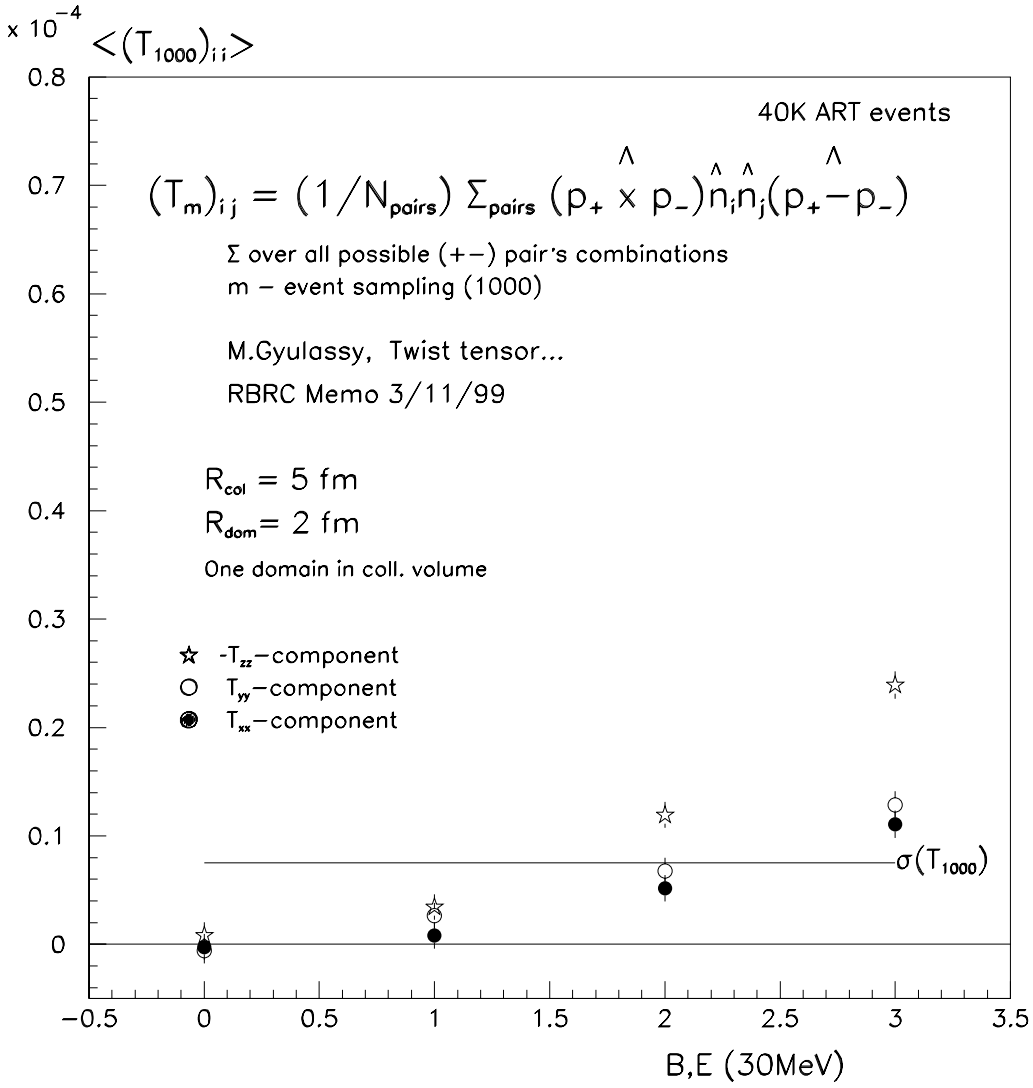

Figure 3.9: The average values of the diagonal elements of $T_{i,j}$ for various factors of the P,T violating fields (in terms of the minimum value). The horizontal line shows the standard deviation of the width of the distribution of averages of 1000 event subsamples, calculated for a total sample of 40,000 events. The vertical lines on the points indicate the standard deviations of the averages.

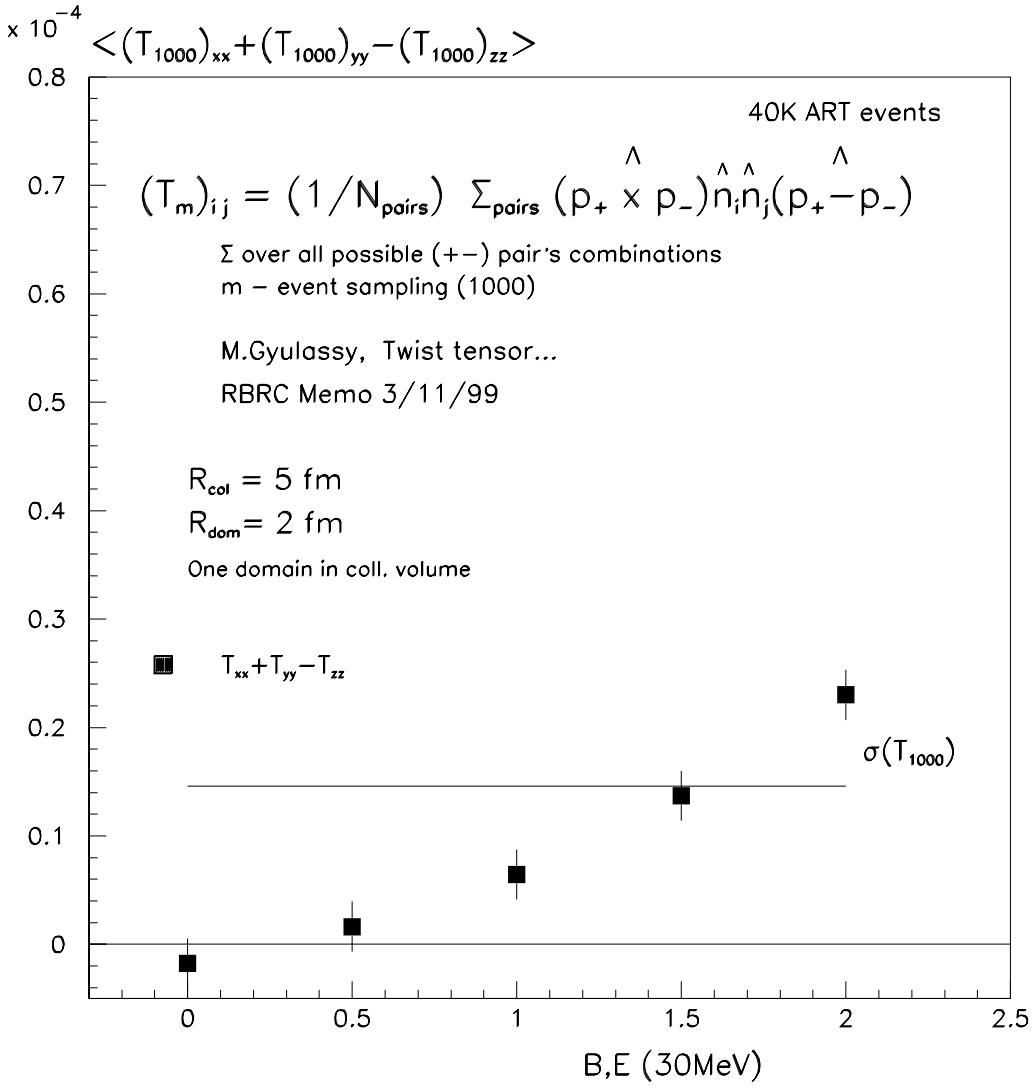

Figure 3.10: The average values of the sum $T_{xx} + T_{yy} - T_{zz}$ for various factors of the P, T violating fields (interms of the minimum value). The horizontal line shows the width of the distribution of averages for 1000 event subsamples, calculated for a total sample of 40,000 events. The vertical lines indicate the standard deviations of the averages.

4. Summary, Twist Tensor Studies

The difference between the fast simulation and HIJING can be viewed as typical of the sensitivity of the measurement to the details of the events that will be produced in central RHIC collisions. We conclude that samples of 40,000 events are close to what is required from a statistical point of view. We also conclude that effects in the twist tensor components can be expected at the few $\times 10^{-6}$ to 10^{-5} level. From this we can conclude that the experimental biases which can create a fake effect must be controlled at the 10^{-6} level or better (in the components of the twist tensor).

In a future note we will analyze the question of experimental biases which could create a fake effect.

5. Kharzeev "Triple Product"

Reference [1] proposes the variable J, defined via:

$$J = (\frac{1}{N_{pairs}}) \sum_{pairs} \frac{\vec{p_+} \times \vec{p_-}}{|\vec{p_+}||\vec{p_-}|} \cdot \hat{\lambda} \tag{5.1}$$

In equation (5.1) $\hat{\lambda}$ is a unit vector in either the x, y, or z direction. As can be seen, J is odd under P but even under C (charge conjugation). If the initial state were an eigenstate of C, the fact that C is conserved (as it is in the theory hypothesized in [1]) would lead to the vanishing of J even if P were violated in the interaction. However, the initial state is not an eigenstate of C and J can show effects of the P violation of [1].

In equation (5.1) the sum extends of all pairs in a given event. We will later extend the definition to include the sum over all pairs in a given size subsample of events. But until further notice, we take the sum over all pairs in a given event.

The symmetries of the interaction are important in using the variable J. Because we assume a collision between identical heavy ions, all particle kinematic distributions must be for/aft symmetric. That is, if θ is the space angle of a particle with respect to one of the beams and $\frac{dN}{d\theta d\phi}$ is the number of a given particle type per unit space angle θ per unit azimuthal angle ϕ, then

$$\frac{dN}{d\theta d\phi}(\theta, \phi) = \frac{dN}{d\theta d\phi}(\pi - \theta, \phi) \tag{5.2}$$

Furthermore, we asume that the beam ions are either spinless or unpolarized. Therefore there will be azimuthal assymettry around the beam axis (which in this note we always take to be the z axis).

$$\frac{dN}{d\theta d\phi}(\theta, \phi) = \frac{1}{2\pi} \frac{dN}{d\theta d\phi}(\theta) \tag{5.3}$$

These two symmetries lead to the vanishing of J, if it is simply calculated as defined. We now demonstrate this and show how to modify the calculation of J to avoid this cancellation.

Let us take the case of $\hat{\lambda} = \hat{x}$ and an effective $\vec{B}$ field also in the $\hat{x}$ direction. Other cases are treated in an exactly similar fashion.

Let the component of $\vec{p_+}$ in the y, z plane be A_t and the component of $\vec{p_-}$ in the y, z plane be B_t. Let the projected angle of $\vec{p_+}$ in the y, z plane be θ_+ and the projected angle of $\vec{p_-}$ be θ_-.

The effect of the (P violating) effective $\vec{B}$ field will be to rotate the projections of $\vec{p_+}$ and $\vec{p_-}$ in the y, z plane by amounts we designate as δ_+ and δ_- respectively. Here we have taken δ_+ and δ_- to both be positive quantities. The proper directions of rotation will be taken into account by appropriately adding or subtracting the magnitudes. Of course, it doesn't matter. Any convention, consistently used would suffice. That is, if the positive and negative particles are produced at θ_+ and θ_-, they will be observed (after passing through the P violating field domain) at

$$\theta'_+ = \theta_+ + \delta_+$$

and

$$\theta'_- = \theta_- - \delta_-$$

Consider one (arbitrary) choice of A_t and B_t. The value of J which will be observed, which we call J', will be given in terms of the original production angles θ_+, θ_-, and the rotations δ_+ and δ_- by:

$$J' = A_t B_t sin(\theta_+ - \theta_- + \delta_+ + \delta_-)$$

The mean value of J' is obtained by integrating J' multiplied by the probability of producing the positive particle at θ_+, $P(\theta_+)$, times the probability of producing the negative particle at θ_-, $P(\theta_-)$.

$$< J' >= \int A_t B_t sin(\theta_+ - \theta_- + \delta_+ + \delta_-) P(\theta_+) P(\theta_-) d\theta_+ d\theta_- \qquad (5.4)$$

We assume that the positive and negative particles are produced in an uncorrelated fashion. Although this may not (indeed, will not) be strictly true, the large particle production at RHIC means that it is almost true. If we have an effect which vanishes when the positive and negative particles are uncorrelated, the effect is almost certainly too small to be visible.

Now the for/aft symmetry and the azimuthal symmetry tells us that the distribution of particles will satisfy: in the y, z plane, i.e.

$$\frac{dN}{d\theta_+}(\theta_+) = \frac{dN}{d\theta_+}(\pi + \theta_+)$$

Because $\frac{dN}{d\theta_+}(\theta_+)$ is modulo 2π, it follows that

$$\frac{dN}{d\theta_+}(\theta_+) = \frac{dN}{d\theta_+}(\theta_+ - \pi)$$

A similar relation obviously holds for $\frac{dN}{d\theta_-}(\theta_-)$ as well.

Remembering that the probability $P(\theta_+)$ is proportional to $\frac{dN}{d\theta_+}(\theta_+)$, we see that each contribution to the integral in (5.4) at $\theta_+ - \theta_- + \delta_+ + \delta_-$ is matched by an equal in magnitude but opposite sign contribution from $\theta_+ - \pi + \theta_- + \delta_+ + \delta_-$. The integral thus vanishes. A similar analysis holds for θ_-, so we conclude:

To see the effects of the P violating $\vec{B}$ field we need to change the sign of the triple product whenever θ_+ and θ_- are of opposite sign.

In the simulations which will be described next this has been done. As will be seen the simulations verify the above analysis.

These simulations were all done with the (so called) fast simulation events. This was necessary to obtain adequate statistics. The tracks were generated as explained in section 2. However, there are two ways we have used the tracks to make pairs. In the first of these, the uncorrelated type, we just pair each positive track with a single negative track, with random association. No track appears in more than one pair. The number of pairs is equal to the number of tracks of whichever sign had the least number of tracks.

The second method, so called correlated sample, proceeded as follows. A positive track is chosen randomly, then a negative "mate" is chosen at random from the set of generated negative tracks. This process is repeated for a total of 10 times the number of positive tracks. However, the resulting pair is discarded if any track in the pair has appeared three times in previously chosen pairs. As it happens, this restriction eliminates only a small fraction of the pairs, so nearly 10,000 pairs are generated in a typical "correlated" event.

At this point we extend the definition of J to include all pairs created in a subsample of a given number of events.

The statistic which we use to describe the behaviour of J, is the fraction of J values which are positive. If P were conseved, the expectation value of J would be zero

and there would be as many positive triple products as negative. We consider the fraction of positive triple products minus 0.5. If the individual triple products are statistically independent, and P is not violated, the number of positive values of J should have mean of 1/2 the total number of products and a standard deviation of $\sqrt{Npq}$, where N is the total number of events and p and q are the probabilities of positive and negative values respectively. The mean value of this statistic for a subsample of N_{sub} events should thus be distributed with a standard deviation $\sqrt{N_{sub}pq}$. Of course for no P violation $p = q = 0.5$.

For pairs which are correlated, the standard deviation (often denoted as "width" here) can be different.

Figure 5.1 shows, for uncorrelated pairs, the distribution of the fraction of J values which are positive less 0.5 in 10 event subsamples, for two cases. The first, has no P violating $\vec{B}$ field and the second has the standard "minimum" value (as defined in section 2) always pointing in the $\hat{x}$ direction. Although this latter case is unphysical, as the field would point in a random direction in each event, this type of plot is useful in understanding the behaviour. In figure 5.1 there are 10^6 events in the uncorrelated sample and $60,000$ events in the correlated sample.

We see that the means of the three variants of J are all zero when there is no field. When the minimum field is present (always in the $\hat{x}$ direction), J_x shows a non zero mean value while J_y and J_z do not. This is just what would be expected from the definition of J and the direction chosen for the field. It should be noted that if we had not reversed the sign of J whenever θ_+ and θ_- had opposite signs, even the J_x distribution would have been centered at zero in agreement with the analysis presented above.

Now we consider the more realistic case where the P violating field points in a random direction in each event. Since on the average the field points equally in all directions, we would not expect a shift in the mean value of J. That is, in an overall average sense there is no P violation. However, the fact that in each event the values of the triple products are slightly shifted by the P violating field means that the width of the J distributions might show an effect. There are two difficulties with this measure of P violation. The first, as we shall see, is that the effect on the width is rather miniscule. This is due to the fact that for each event, the contribution to the width from the P violating field adds in quadrature with the statistical width $(\sqrt{Npq})$.

The second is that we do not know, a priori, what the width should be in the absence of P violation.

The size of the effect is illustrated by figure 5.2 which shows the distributions of the

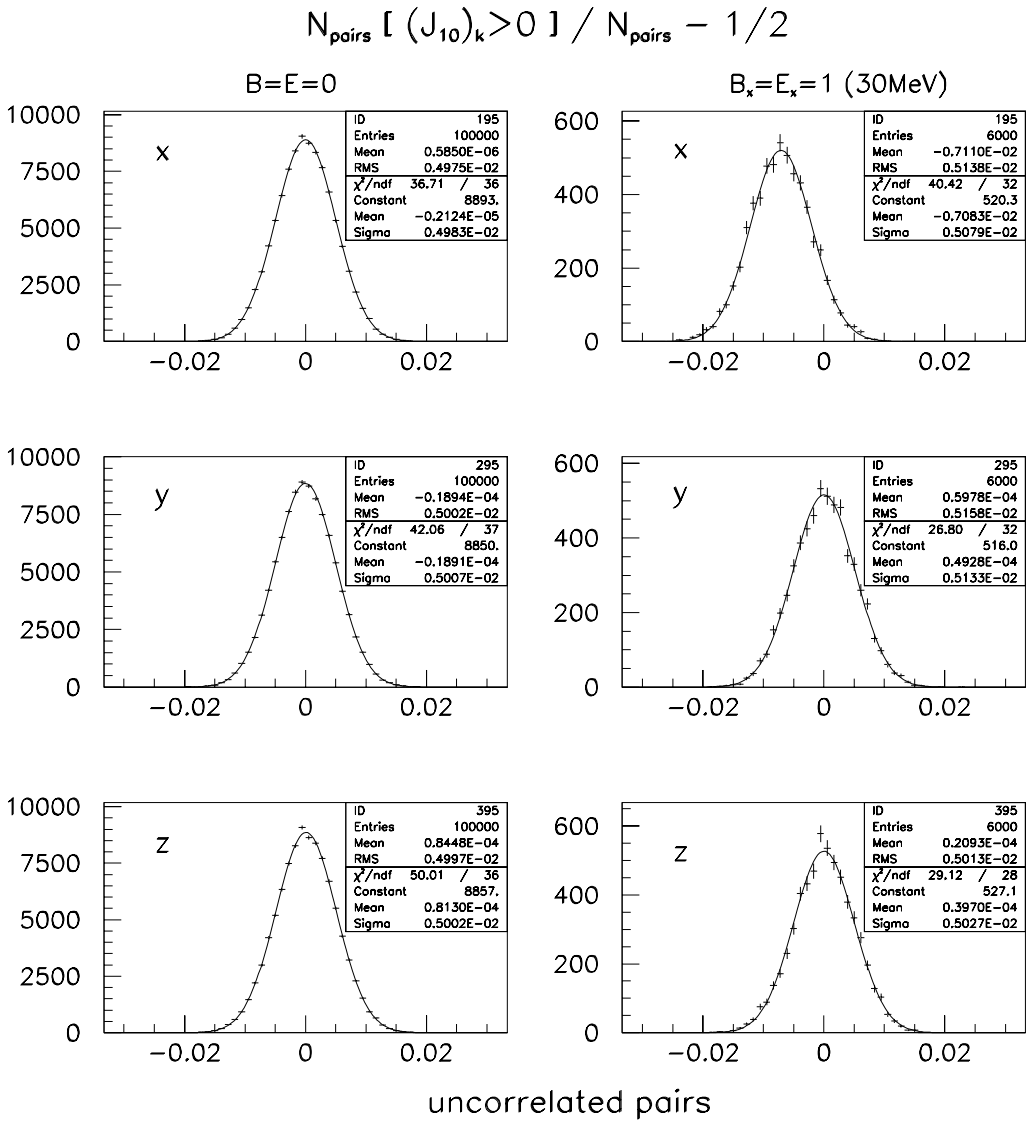

Figure 5.1: The distribution of the fraction of J values in 10 event subsamples, for uncorrelated pairs, which are positive. The left hand plot for no P violating field and the right hand plot for a field of $3\times$ the minimum value (see section 2) always pointing in the $\hat{x}$ direction.

fraction of J values, for 1000 event subsamples, which are positive. Results with uncorrelated and correlated pairs are shown. To amplify the effect, the value of the P violating field has been chosen as $3\times$ the minimum value.

As expected, the distributions all peak at zero. The widths of the correlated and uncorrelated samples are rather similar despite the fact that there are about $10\times$ more pairs per event in the correlated sample.

Finally, using our model of the phenomenon we have calculated the effect on the width of varying the strength of the P violating field. By comparing the width with zero field with the width with, say, the minimum field, we can estimate the size of the influence on the width caused by the P violating field. The results are shown in figure 5.3. Figure 5.3 shows, for both correlated and uncorrelated samples, the width calculated with varying values of the P violating field.

For the uncorrelated sample 10^6 events were used and for the correlated sample 200×10^3 events were used. There are of course, approximately $10\times$ as many pairs per event in the correlated sample as in the uncorrelated one. Figure 5.3 shows the width of the distribution of the fraction of J (with $\hat{x}$, $\hat{y}$, and $\hat{z}$) for a 1000 event subsample which are positive. The horizontal lines show the expected width, assuming the individual triple products are statistically independent.

For the uncorrelated sample there is essentially no effect at a level detectable with 10^6 events. The width, as expected, is in agreement with the theoretical value. For the correlated sample, there is a slight dependence, not quite significant at the 200×10^3 level. The width is considerably larger than expected from the statistically independent assumption. This is reasonable since many of the pairs in the correlated sample share a common track and hence are not statistically independent. Of course, to simulate the effect which might be observed, the direction of the field is chosen randomly for each event.

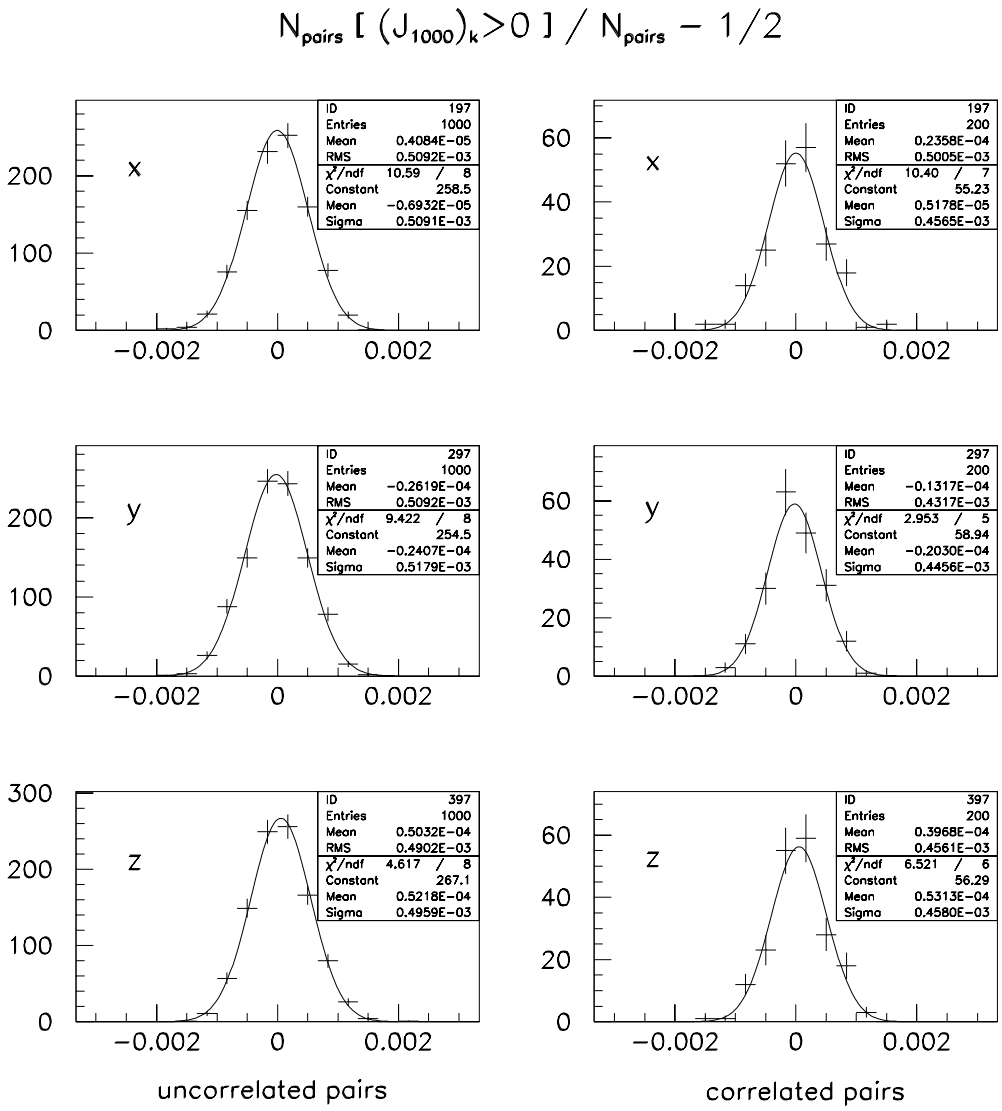

Figure 5.2: The distribution of J values for 1000 event subsamples for the case in which the P violating field is $3\times$ the minimum value and is randomly oriented in each event. The left plots show the results for uncorrelated pairs and the right plots for correlated pairs. The direction of the field is chosen randomly in each event.

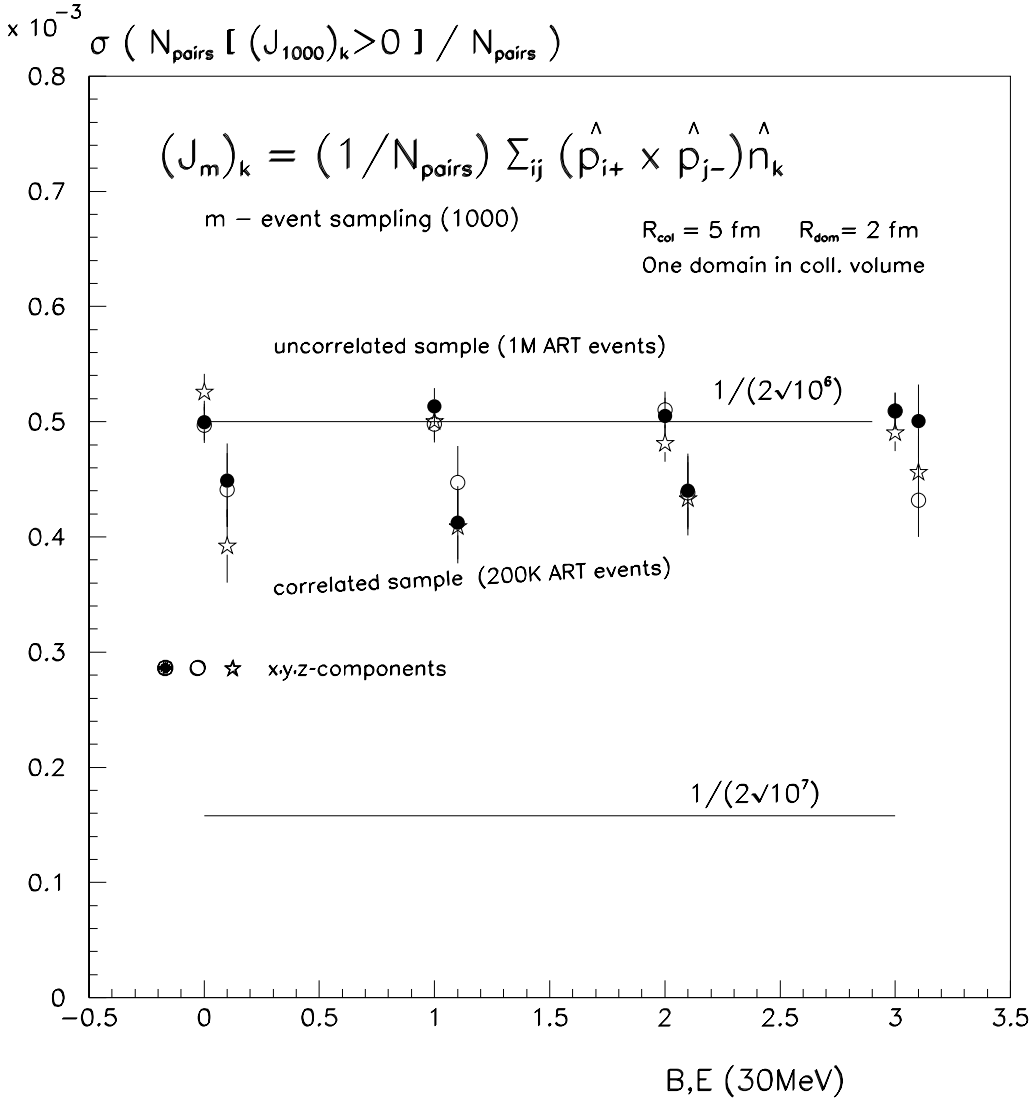

Figure 5.3: The values of the width of the distribution of the fraction of J values which are positive as a function of the P,T violating field. The three types of J are shown as indicated on the figure. Both correlated and uncorrelated samples are shown. The horizontal lines show the expected widths if the individual triple products were statistically independent. Of course, the direction of the P violating field is chosen randomly in each event.

6. Summary of The Kharzeev " Triple Product" Parameter

The results of the previous section show that the Kharzeev triple product parameters are not promising parameters for the study of the possible P, T violating effects. This is because the field points in a different direction in each event so the only way to use a large sample of events is to seek effects on the widths of J distributions. This in turn has the serious difficulty that, at least at the start of RHIC studies, we have no way of estimating what the widths should be in the absence of P,T violating effects. Furthermore, the effects on the width appears to be rather minor.

7. JJ Parameter

In an attempt to find a parameter which is additive from event to event, we have examined a parameter we call JJ. In a given event there is a greater probability that an individual triple product will have given sign. Thus for the pairs in a single event we are more likely to find $++$ or $--$ than we are to find $+-$ or $-+$.

This led us to define the parameter JJ defined as follows:

$$JJ = (\frac{1}{N_{doublets}}) \sum_{i,j} (\frac{\vec{p_+} \times \vec{p_-}}{|\vec{p_+}||\vec{p_-}|} \cdot \hat{\lambda})_i (\frac{\vec{p_+} \times \vec{p_-}}{|\vec{p_+}||\vec{p_-}|} \cdot \hat{\lambda})_j \tag{7.1}$$

In equation (7.1) the $N_{doublets}$ refers to the number of pairs of pairs used in calculating the parameter JJ. The choices are made in two different ways which will be explained below.

The parameter JJ is additive but it has the disadvantage that it is not a P odd parameter so it may have a nonzero value even if P is not violated. However, it may be possible to estimate what JJ would be if P were not violated, so it might turn out to be a useful parameter and we study it with our simulation.

For all of these studies we use the fast simulation events. In the so-called uncorrelated choice, we take the pairs generated in the uncorrelated fashion as explained in section 2 (no pair contains a track which occurs in any other pair, i.e. pairs have no tracks in common). For these pairs we form pair doublets with no doublet having a pair which occurs in any other doublet. So if we had 1000 positive tracks and 1000 negative tracks, we would form 1000 uncorrelated pairs. Of these we would then form 500 uncorrelated pair doublets. These doublets are then used to form the JJ parameter for the event or for a subsample of such events. The $N_{doublets}$ is the number of doublets used, either the number in the event or the number in the subample of events as the case may be.

In the so-called correlated sample we start with the correlated pairs (as discussed in section 2). Then in a random fashion we try to form a number of pair doublets of $10\times$ the number of pairs but exclude duplicate doublets. We thus typically form

somewhat fewer than 10^5 such doublets per event. These doublets are then used to form the JJ parameter for the event or for the subsample of events.

As we did for the Kharzeev triple product, we use as a statistic, the fraction of JJ which are positive minus 0.5. Since JJ is not P odd this can have a nonzero mean for a subsample. Although of course, for the uncorrelated sample it should have a zero mean.

Figure 7.1 shows the distribution of this statistic for 1000 event subsamples for the correlated and uncorrelated cases for the P violating field taken at $3\times$ the minimum value. The field is, of course, chosen to be in a random direction in each event.

Figure 7.2 shows the mean values of the fraction of positive JJ (minus 0.5) as a function of the magnitude of the P violating field for 1000 event subsamples. For the oncorrelated case a total of 10^6 events were used and for the correlated case 200×10^3 events were used.

We can see that the effect is very small. In the uncorrelated case, the effect is not visible with 10^6 events. For the correlated case the mean value is shifted from zero but as seen from figure 7.2 it is mostly due to the correlations between the particles in the event and only slightly due to the P violating field. This is shown by the small value of the shift of the parameter with the magnitude of the P violating field.

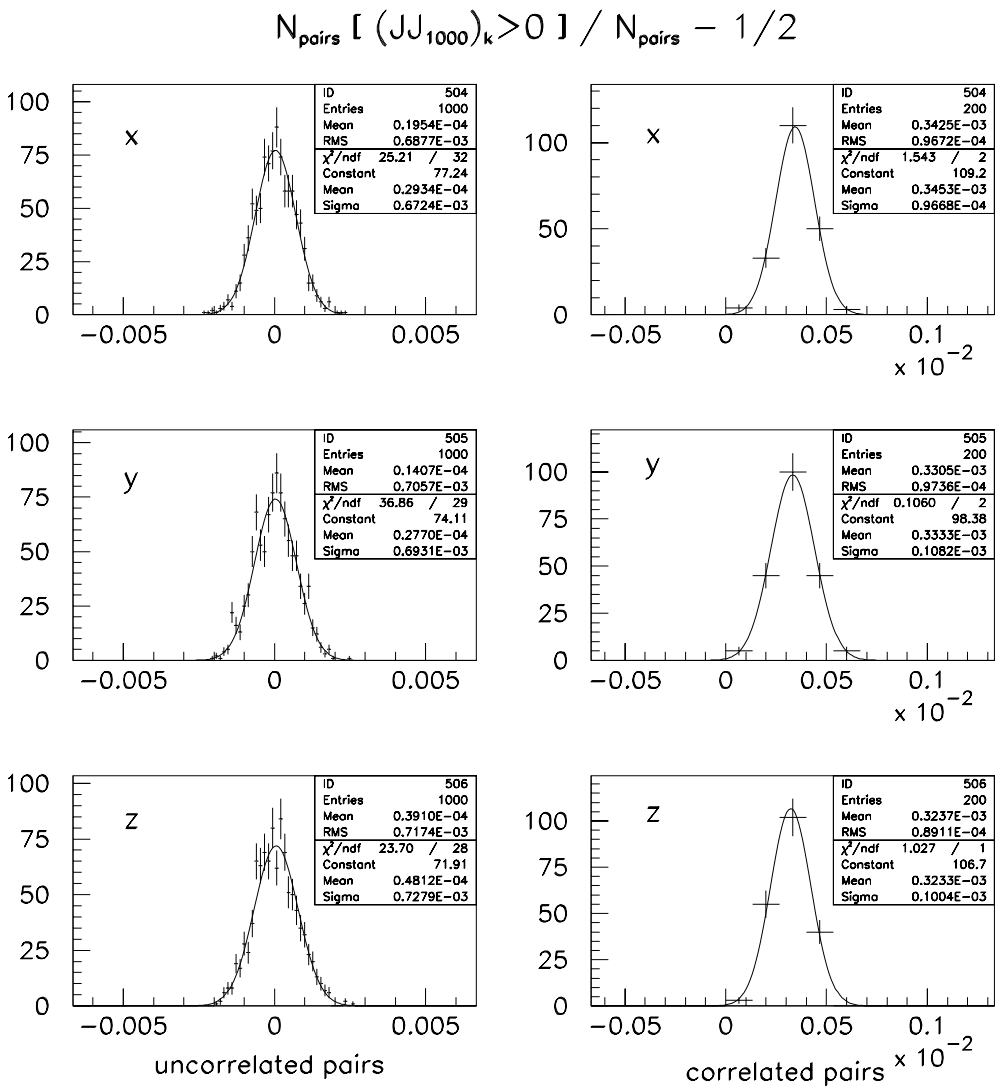

Figure 7.1: The distribution of the fraction of JJ which are positive minus 0.5, for 1000 event subsamples, for the correlated and uncorrelated cases (see text for further explanation) The direction of the P violating field is chosen randomly in each event.

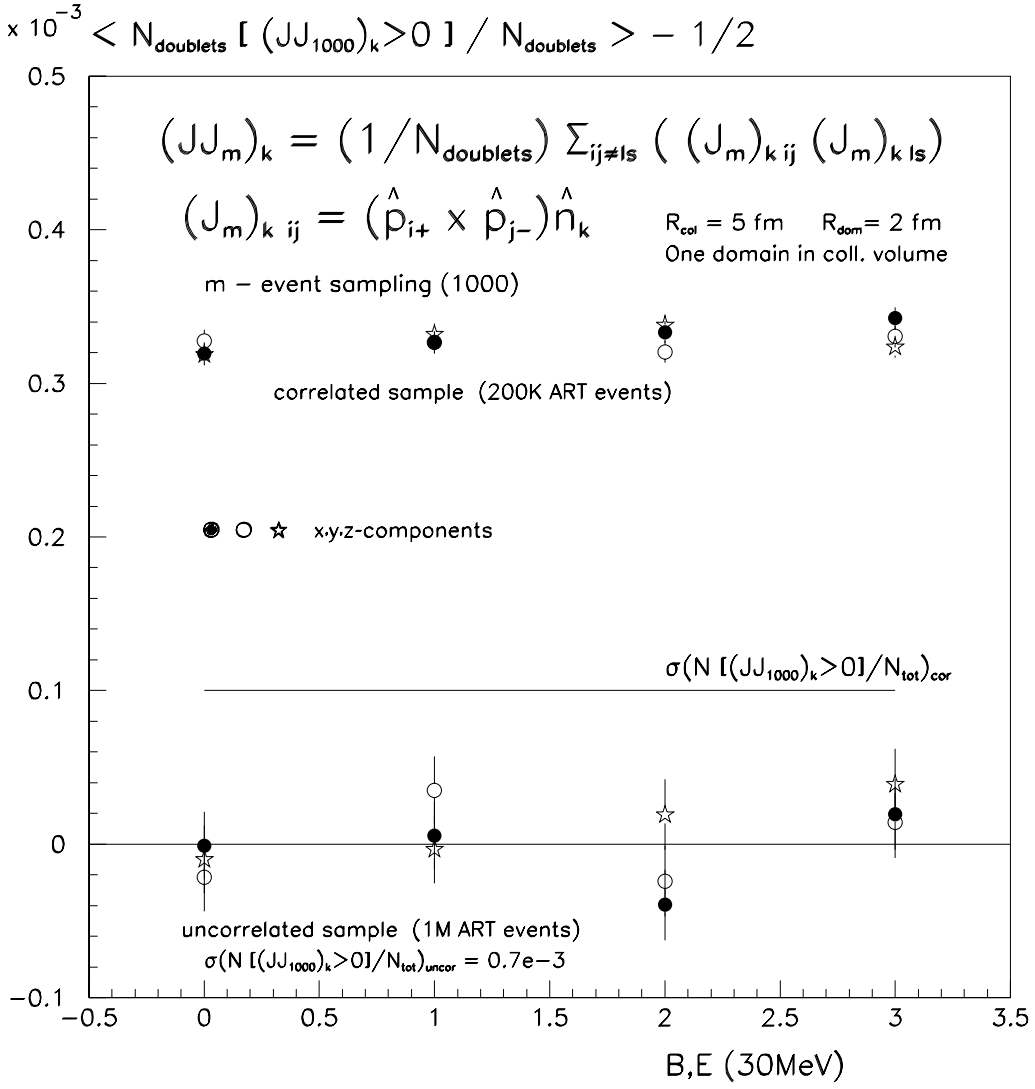

Figure 7.2: The mean value of the fraction of positive JJ (minus 0.5) , for 1000 event subsamples, as a function of the magnitude of the P violating field for the correlated and uncorrelated cases. The direction of the P violating field is chosen randomly in each event.

8. Summary of the JJ Parameter Studies

Unfortunately, we conclude that the JJ parameter, like the Kharzeev triple product parameter, is not a promising parameter to use for the search for P, T violating effects in the RHIC collisions.

Bibliography

[1] D. Kharzeev, R.D. Pisarski, and M.H.G. Tytgat, Phys. Rev. Lett. 81, 512 (1998)

[2] D. Kharzeev, private communication

[3] M. Gyulassy, RBRC MEMO 3/11/99

[4] Instructions for subscribing are given at http://www.ccd.bnl.gov/mail/listproc

[5] http://www.rhic.bnl.gov/~jhthomas/parity